NASA/TM-20205006994

An Algorithm for Characterization of Fiber Aggregation in Composite Microstructures

Jamal F. Husseini and Scott E. Stapleton
University of Massachusetts Lowell, Lowell, Massachusetts

Evan J. Pineda
Glenn Research Center, Cleveland, Ohio

December 2020

NASA STI Program . . . in Profile

Since its founding, NASA has been dedicated to the advancement of aeronautics and space science. The NASA Scientific and Technical Information (STI) Program plays a key part in helping NASA maintain this important role.

The NASA STI Program operates under the auspices of the Agency Chief Information Officer. It collects, organizes, provides for archiving, and disseminates NASA's STI. The NASA STI Program provides access to the NASA Technical Report Server—Registered (NTRS Reg) and NASA Technical Report Server—Public (NTRS) thus providing one of the largest collections of aeronautical and space science STI in the world. Results are published in both non-NASA channels and by NASA in the NASA STI Report Series, which includes the following report types:

- TECHNICAL PUBLICATION. Reports of completed research or a major significant phase of research that present the results of NASA programs and include extensive data or theoretical analysis. Includes compilations of significant scientific and technical data and information deemed to be of continuing reference value. NASA counter-part of peer-reviewed formal professional papers, but has less stringent limitations on manuscript length and extent of graphic presentations.

- TECHNICAL MEMORANDUM. Scientific and technical findings that are preliminary or of specialized interest, e.g., "quick-release" reports, working papers, and bibliographies that contain minimal annotation. Does not contain extensive analysis.

- CONTRACTOR REPORT. Scientific and technical findings by NASA-sponsored contractors and grantees.

- CONFERENCE PUBLICATION. Collected papers from scientific and technical conferences, symposia, seminars, or other meetings sponsored or co-sponsored by NASA.

- SPECIAL PUBLICATION. Scientific, technical, or historical information from NASA programs, projects, and missions, often concerned with subjects having substantial public interest.

- TECHNICAL TRANSLATION. English-language translations of foreign scientific and technical material pertinent to NASA's mission.

For more information about the NASA STI program, see the following:

- Access the NASA STI program home page at http://www.sti.nasa.gov

- E-mail your question to help@sti.nasa.gov

- Fax your question to the NASA STI Information Desk at 757-864-6500

- Telephone the NASA STI Information Desk at 757-864-9658

- Write to:
  NASA STI Program
  Mail Stop 148
  NASA Langley Research Center
  Hampton, VA 23681-2199

NASA/TM-20205006994

An Algorithm for Characterization of Fiber Aggregation in Composite Microstructures

Jamal F. Husseini and Scott E. Stapleton
University of Massachusetts Lowell, Lowell, Massachusetts

Evan J. Pineda
Glenn Research Center, Cleveland, Ohio

National Aeronautics and
Space Administration

Glenn Research Center
Cleveland, Ohio 44135

December 2020

Acknowledgments

This work was supported by the NASA Lewis' Educational and Research Collaborative Internship Project (LeRCIP) at the Glenn Research Center. The authors would like to acknowledge and thank the Air Force Research Laboratory for very detailed composite microstructure images. The authors would like to also thank Brett Bednarcyk at NASA Glenn for support and feedback on developing this program as well as Matt Schey, University of Massachusetts Lowell, for helping with MATLAB® coding.

Level of Review: This material has been technically reviewed by technical management.

Available from

NASA STI Program
Mail Stop 148
NASA Langley Research Center
Hampton, VA 23681-2199

National Technical Information Service
5285 Port Royal Road
Springfield, VA 22161
703-605-6000

This report is available in electronic form at http://www.sti.nasa.gov/ and http://ntrs.nasa.gov/

An Algorithm for Characterization of Fiber Aggregation in Composite Microstructures

Jamal F. Husseini and Scott E. Stapleton
University of Massachusetts Lowell
Lowell, Massachusetts 01854

Evan J. Pineda
National Aeronautics and Space Administration
Glenn Research Center
Cleveland, Ohio 44135

Abstract

Composite structures are susceptible to localized flaws, or variability, that drive global failure. To capture this variance, a multiscale model needs to be introduced that not only accurately represents the statistical nature of the composite microstructure but is also efficient. At the microscale, fiber aggregation creates local stress concentrations, where failure is likely to occur sooner than expected. A method of rapid microstructure generation, in conjunction with cluster characterization, is examined to develop accurate reproductions of 2D composite cross-sections. Parameterization of shape and size of fiber clusters is used to characterize representative volume elements. The discrete element method is used to generate pseudo-microstructures. The clustering parameters from the pseudo- and actual microstructure arrangements (obtained from micrographs) can be compared to determine the validity of the representative volume element generated with the discrete element method. Results show a promising approach to evaluating randomness of fiber distributions and how to accurately recreate microstructures for strength analysis.

1.0 Introduction

Key geometrical and material characteristics must be taken into consideration when predicting strength and overall response of composites under loading (Refs. 1 to 3). One important abnormality in fiber reinforced composites to consider is microscale fiber clustering (Refs. 4 and 3). Herein, fiber clustering is defined as deviation from homogeneity in spatial distributions, leading to aggregations of points or associated fibers (Ref. 5).

Local fields are not captured accurately in many finite element models of representative volume elements (RVEs) of composites due to the extensive computation time needed to sufficiently capture the driving factors that initiate failure from close/ touching fibers with a suitable mesh (Refs. 5 and 6). The assumptions often utilized in homogenization are that the fibers are continuous, do not bend or kink, and are arranged uniformly in hexagonal packing within a repeating unit cell (RUC) so that the average fiber volume fraction of the composite is captured.

An image taken from a scanning electron microscope (SEM) of a composite microstructure can be seen in Figure 1(a). It can be seen there are regions that have homogenous fiber arrangement (Figure 1(c)), to resin-rich areas between groupings of fibers (Figure 1(b)), as well as fibers that are very close or touching exhibiting extreme deviation from homogenous distribution (Figure 1(d)). In the latter case, it is very difficult to discern whether the matrix between fibers has voids or altered material properties from curing. A visual examination makes it difficult to detect these anomalies which could be critical for the onset of matrix cracking.

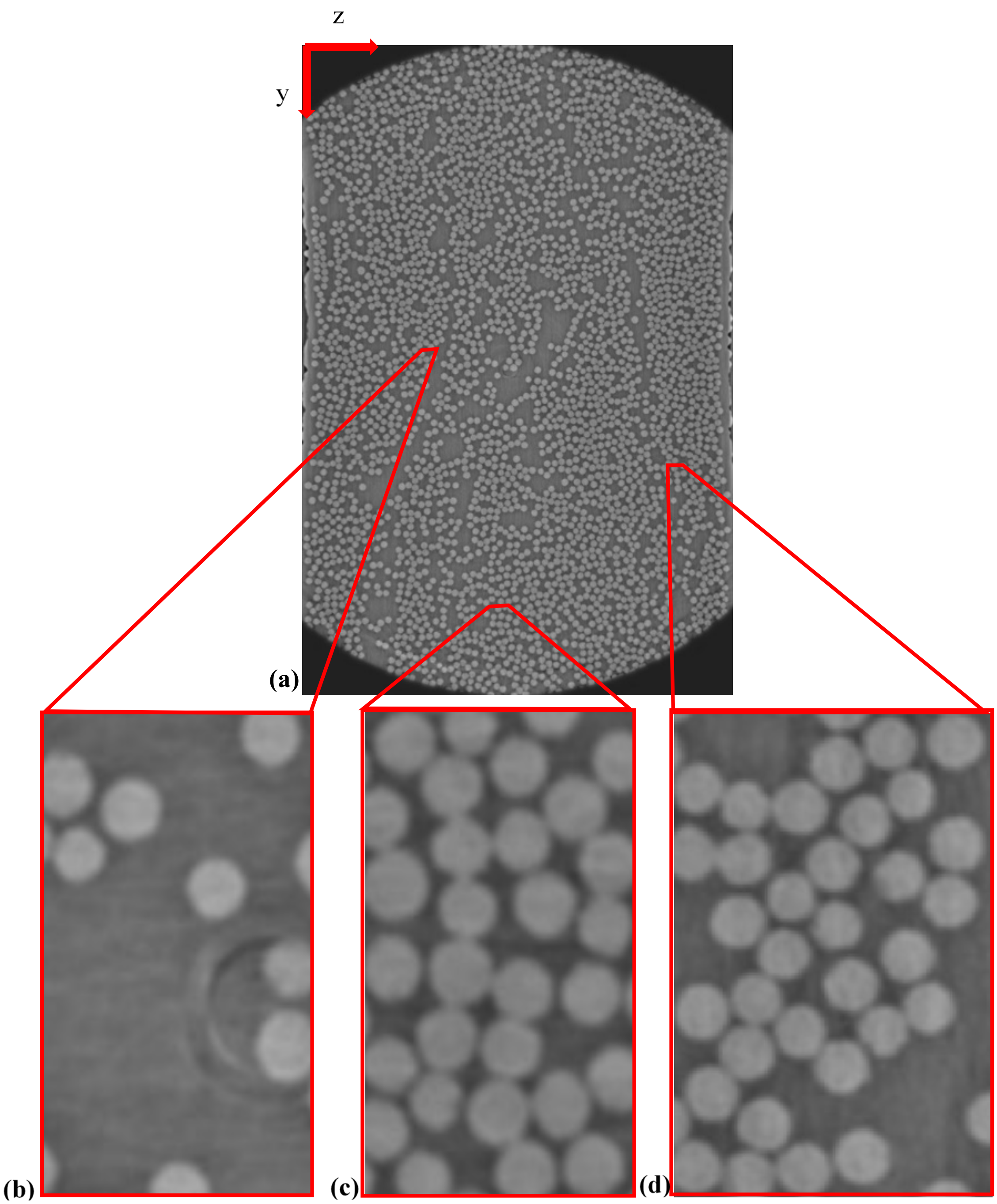

Figure 1.—(a) SEM image of the microstructure of a fiber reinforced composite used in automotive applications. (b) Resin-rich region. (c) Homogenous section where fibers are arranged consistently. (d) Clustered section where fibers are grouped such that they are close or touching.

In order to simulate this randomness, the current approach utilizes the discrete element method (DEM) where fibers are randomly placed in cells and undergo a relaxation through energy damping (Ref. 7). The magnitude of damping is defined by the user and controls the degree of cohesion between fibers. Another advantage of this method is being able to create larger RVEs with higher fiber volume fractions at faster speeds than the traditional method of randomly placing fibers in a fixed-size box. The repeatability of this process, as well as the unique parameterization, allows for simulating the effects of fiber clustering on similar microstructures that exhibit similar characteristics (i.e., number of clusters and cluster size). A portion of the present work aims at relating how the DEM parameters correlate to clusters formation, ultimately providing a method for determining settings to obtain a desired microstructure output.

Many methods have been employed to characterize clustering and the overall global impact it may have on the microstructure (Ref. 1). The most common methods used for determining fiber distributions are Ripley's K Function (Refs. 8 and 9), and corresponding functions to Ripley's such as the L Function, Matérn's Hard-Core Process, and Pair Distribution Functions (Refs. 10 to 12). While many of these statistical measures are beneficial due to their robustness, quick run time, and easy visual interpretation, the designed purpose is to compare the accuracy of distribution in generated samples to real microstructures (Refs. 13 to 16). These statistical measures, such as the K Function, operate by expanding concentric circles around a fixed random point. The K Function is calculated as a function of increasing window radius, which is compared against a Poisson Distribution that represents complete spatial randomness. Complete spatial randomness is a descriptor that compares how often and how many fiber centers are captured as the scanning window radius increases and represents the theoretical value for a random distribution, deviation is an indication of clustering or dispersion. Microstructure fiber distribution is characterized based on how the K Function deviates from the Poisson Distribution, but only from one fixed location. In order to evaluate an entire microstructure, the process must be executed from multiple fixed points, all comparing different window sizes. Fixing the window size and performing one calculation at points that cover the RVE, multiple values can be compared against a theoretical limit for determining high fiber aggregation.

By scanning for local regions of high fiber density, cluster size and shape can now be determined and quantified. The objective of this work is to utilize a method of rapid generation of fiber reinforced composite RVEs and a new method for quick evaluation of localized fiber clustering. A DEM program is used with different input parameters that change the effect of clustering in microstructures containing 225 fibers at a volume fraction of 40 percent. To identify clustering, a method of local volume fraction calculation was conducted, followed by a cutoff evaluation to determine which fibers are part of a cluster. All fibers will be connected using Delaunay Triangulation to form a cluster geometry and filtered based on neighboring fibers. The output of this algorithm will be a total number of clusters per RVE and the ratio of cluster area to RVE area. Multiple simulations will be conducted to examine the effect of different DEM inputs and the resulting cluster characteristics.

2.0 Method

In order to recreate random fiber clustering in a microstructure, a computational method, using DEM, will be used to rapidly generate random RVEs. In addition, an algorithm has been developed that scans for high localized volume fractions based as a means of identifying and characterizing fiber aggregation. Inputs to this analysis are RVE size, number of fibers, and global volume fraction.

2.1 Generation of Composite Microstructures Using the Discrete Element Method

The DEM can be used to generate disordered composite microstructures by randomly placing a specified number of fibers in a cell with a fixed number of total cells in the sample. Before the process starts, the amount of overlap each fiber has will result in a certain amount of energy the fibers will move with. Once the process starts, the sample will undergo a relaxation period where collisions of fibers will result in a random placement. Kinetic energy is tracked and eventually will reach a significant point where relaxation ends. Assumptions of the DEM for microstructure generation include that the fibers are parallel and treated in a line mass (Ref. 17). Governing physics and equations of DEM can be examined more closely in References 18 and 19.

2.1.1 Contact Damping

As the sample undergoes relaxation, the fibers will come to rest based on the amount of energy damping. For this study, the main damping mechanism being controlled is the amount of contact damping. Contact damping controls the amount of energy dissipated when fibers collide with each other. Losing more energy rapidly will cause the fibers to stick together and clustering will occur.

2.2 Volume Fraction Scan

In order to determine localized areas of high fiber volume fractions (i.e., clusters), a method of scanning the microstructure is introduced. At each grid location, the fiber volume fraction is calculated and assigned to its respective grid point. To visualize distributions, local volume fraction is interpolated between calculated grid points and a surface is generated. Presented in Figure 2 is a visualization of the microstructure using a grid scanning pattern where the RVE is broken into equally spaced points and a calculation is performed at each fiber center.

The grid method of scanning provides the benefit of refining the resolution by decreasing the distance between y and z grid lines. The scanning window shape and size are presented in Section 2.2.1. Granted, improving the resolution significantly increases the amount of calculations. Convergence studies would need to be performed on each sample to ensure the resolution is fine enough to capture fiber locations. Without refining an optimized grid spacing, the high resolution may lead to higher computation time without improving accuracy of the scan. The distribution plot shown in Figure 2 is not completely smooth and portrays small peaks that correlate to the location of the centers of the fibers.

A method of scanning where the local fiber volume fraction is calculated within windows surrounding each fiber is utilized, such as in Figure 3. Each local volume fraction is assigned to the fiber where the window is centered, and for visualization purposes interpolated between fiber centers to create a surface distribution. Centering the volume fraction calculation around fiber centers ensures there will always be at least one full fiber within the window. Taking calculations at each fiber center results in a smoother distribution than Figure 2, while maintaining a high enough resolution to capture areas of high localized volume fractions. In addition, with the grid methods of scanning, calculation and scan accuracy is a function of chosen grid spacing. Whereas, this method is only dependent of the number of fibers in the RVE. Accuracy is maintained because the calculation still captures all the fibers that have volume within the sample. Inherently, there will be more calculations performed where fibers are close together. As RVE size is increased, the method utilizing fibers as will maintain efficient run time by not performing unnecessary calculations in regions where there are no fibers.

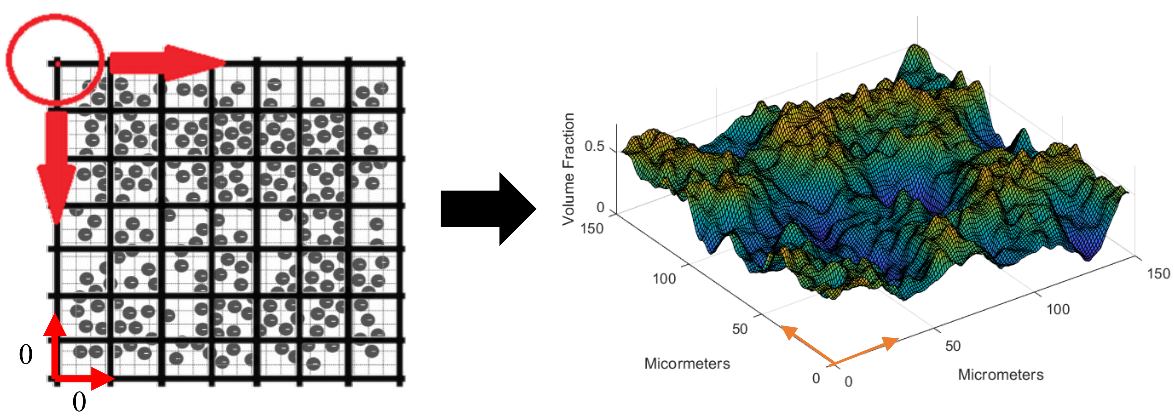

Figure 2.—Grid method of evaluating local volume fractions in the microstructure and resulting plot of volume fraction distribution over RVE area.

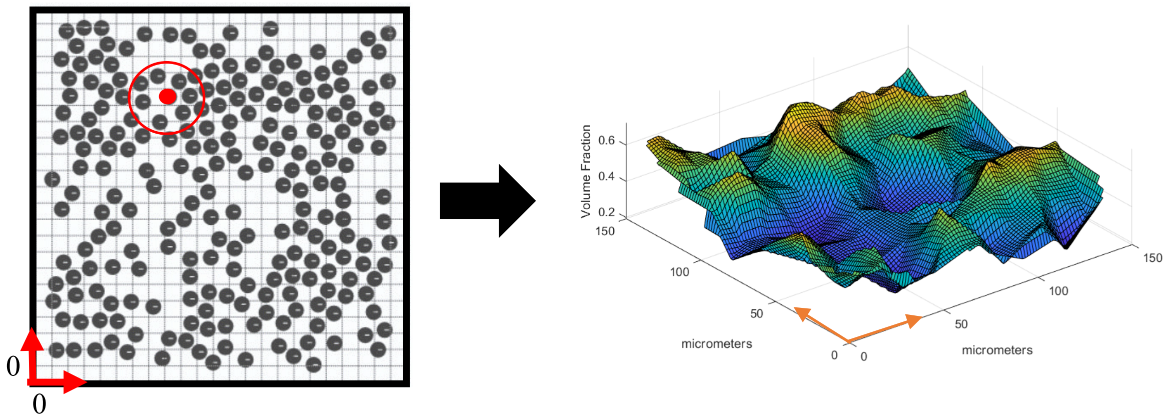

Figure 3.—Fiber center method of evaluating microstructure local volume fractions and resulting plot of volume fraction distribution over RVE area.

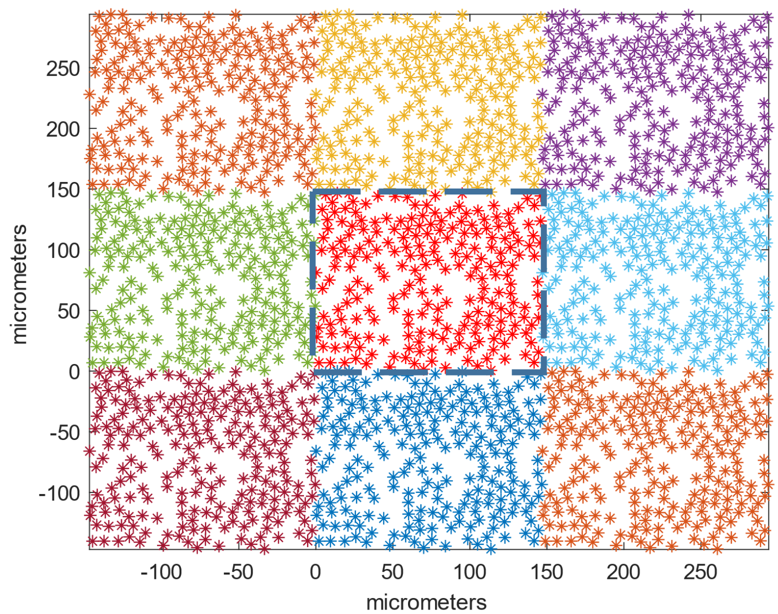

Figure 4.—The central cell (dashed) is the RVE that is analyzed with repeating boundary conditions.

The microstructures shown in both Figure 2 and Figure 3 were used to demonstrate two scanning methods that will later be used to identify fiber clustering. However, periodicity of the microstructure was not enforced. Both DEM and the cluster algorithm, be presented later, incorporates periodic boundary microstructure. Geometric periodicity is enforced by tiling the same microstructure across the boundaries as shown in Figure 4.

2.2.1 Calculating Local Fiber Volume Fraction and Scanning Window Size

Statistical descriptors of fiber distributions, such as the K-function, utilize a growing window size, whereas this method uses a fixed window size that moves across (scans) a sample (Refs. 11, 13, and 14). Window shapes can be circles, squares, etc. but for this study the window is a circle with radius ρ. The results are very sensitive to the size of the scan window. If chosen too small, the window will only be able to capture one fiber; and thus, will exhibit a high-volume fraction. If chosen too large, the window will capture a majority of the sample and the distribution will approach the global, average volume fraction and will not provide statistics on local fiber aggregation.

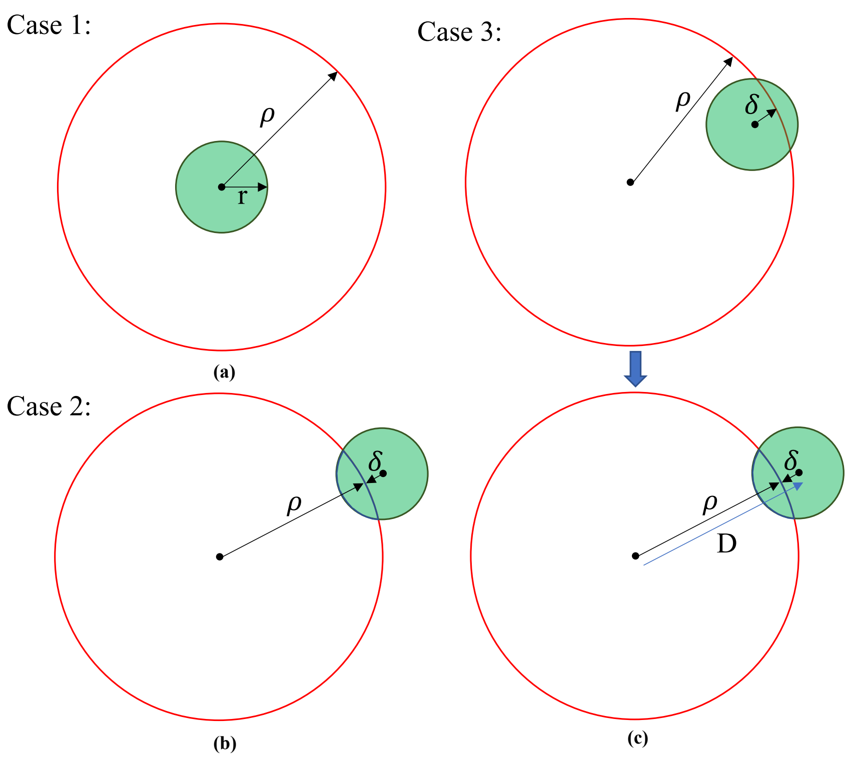

Figure 5.—(a) Case one, (b) case two, and (c) case three of fiber area calculations for local volume fraction. The outer circle (red) is the scanning window, the smaller circle (black) is the fiber radius, and the filled region (green) is the area calculation.

The local fiber volume fraction is calculated dividing the area of all the fibers within the scanning window by the total area. There are three possible cases for the fiber position which affects the volume fraction calculation, see Figure 5. In the first case, shown in Figure 5(a), the entire volume of a fiber i lies within the window, and the area of the fiber cross-section is A_f^i,

$$A_f^i = \pi r_f^2 \tag{1}$$

Since every local volume fraction is sampled at a fiber center, there will be at least one full fiber within the window boundary. Figure 5(b) shows the second case where the fiber center lies outside the window, but part of the fiber is still captured. To calculate the area of fiber i that lies within the window, accounting for the overlapping circular sections, requires the calculation of the fiber sectors.

$$x = \frac{\rho^2 - r_f^2 + D^2}{2D} \tag{2}$$

$$y = \sqrt{\rho^2 - x^2} \tag{3}$$

Then, the area A_f^i is calculated as

$$A_f^i = \rho^2 \sin^{-1}\left(\frac{y}{\rho}\right) + r_f^2 \sin^{-1}\left(\frac{y}{r_f}\right) - y\left(x + \sqrt{r_f^2 - \rho^2 + x^2}\right) \tag{4}$$

where D is the distance between the centers of the window and fiber. The last case (Figure 5(c)) is where a fiber center lies within the scanning window, but part of the fiber lies outside the window. This calculation is performed by subtracting the distance between fiber center and the perimeter of the window and then reflecting the fiber over the window boundary by the same amount, as shown in Figure 5(c).

$$D = \rho + \delta \tag{5}$$

The area of the fiber *i* that lies within the window is calculated by using Equation (5) in Equation (2) and subtracting Equation (4) from the total area of the (Equation (1)).

$$A_f^i = \pi r_f^2 - \rho^2 \sin^{-1}\left(\frac{y}{\rho}\right) - r_f^2 \sin^{-1}\left(\frac{y}{r_f}\right) + y\left(x + \sqrt{\rho^2 - r_f^2 + x^2}\right) \tag{6}$$

The sum of all area parts calculated using Equations (1), (4), or (6), of the total number of fibers that have area inside the scan window n_f yields the total fiber area A_f.

$$A_f = \sum_{i=1}^{n_f} A_f^i \tag{7}$$

Scanning window area can be expressed using Equation (7) as

$$A_w = \pi\rho^2 \tag{8}$$

and the volume fraction captured by that window is

$$V_f = \frac{A_f}{A_w} \tag{9}$$

The closest form fibers can take is HCP which yields volume fraction is ~90 percent. The center to center distance of adjacent fibers is 2r where r is the fiber radius (Figure 6(a)). As the fibers start to disperse from the center fiber, the local volume fraction of the unit cell will decrease and eventually reach the same volume fraction of the RVE. In this scenario, the center to center distance of the fiber is R. The average fiber volume fraction of the RVE, that is to be characterized for clustering, can be used to define the scanning radius of the scanning window ρ = R (Figure 6(b)). This window size is sufficiently large to locate localized volume fractions. In addition, this eliminates the arbitrariness of the window radius as it is based on the minimum window size needed to accurately calculate to local volume fraction in a perfectly ordered (zero clustering) RVE.

Assuming ρ = R, the scanning window radius ρ is dependent on fiber radius and desired volume fraction such that homogenous fiber spacing is

$$R = \sqrt{\frac{2\pi r_f^2}{V_f\sqrt{3}}} \tag{10}$$

where r_f is the fiber radius and V_f is the desired volume fraction.

2.3 Cut-off Value and Clustered Points

Similar to defining the scanning window size, a cut-off value for the local V_f, is defined as the global RVE volume fraction. If a local fiber volume fraction of a window is found to be above the cutoff, the fiber that is used to define the center of the window will be filtered into a group of possible clustered points.

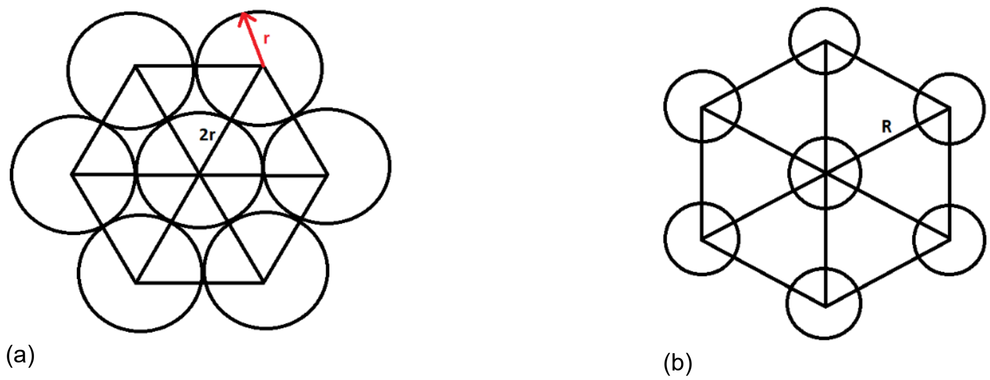

Figure 6.—(a) Hexagonal Close Packed fiber arrangement where the distance between fiber centers is 2r. (b) A homogenous fiber distribution at new distance between points R, used for the scanning window radius.

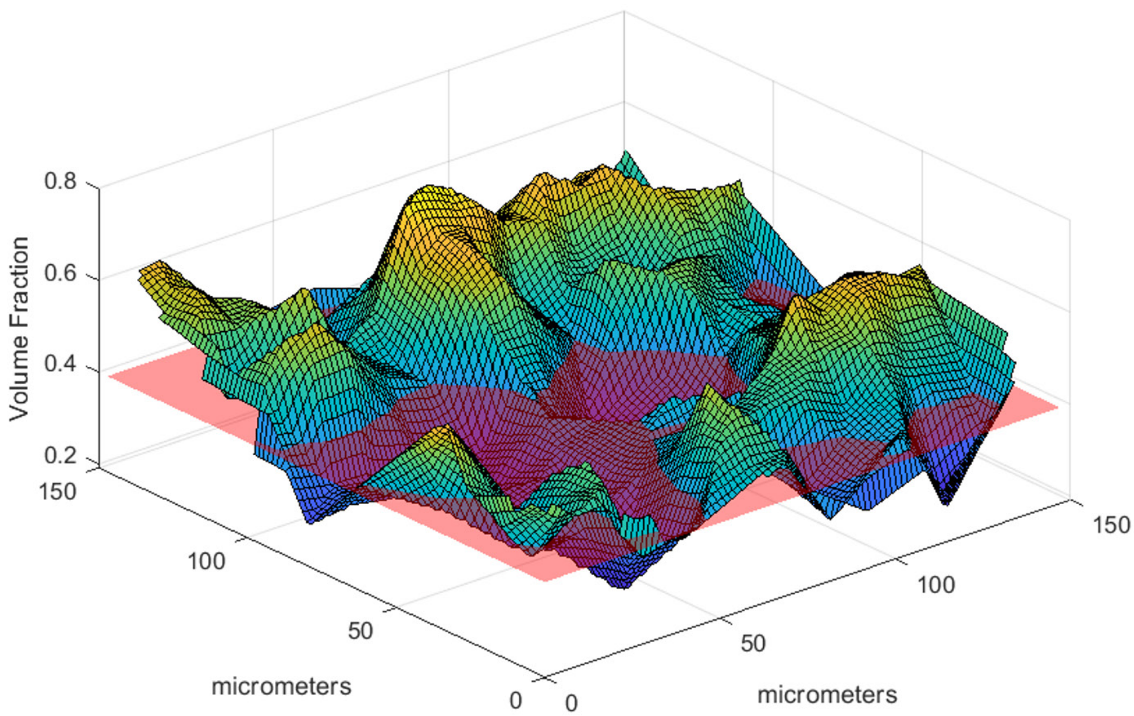

Figure 7.—Visualization of cut-off value (plane) for a sample with a global volume fraction of 40 percent.

The cutoff defined in Figure 7 shows large, connected groups of localized high volume fractions which corresponds to fiber dense regions within the RVE. Any value below the cutoff plane represents fiber dispersion and will only be stored for filtering in the next process step.

2.3.1 Filtering

Only taking fibers that fall above the cutoff still introduces noise due to unpredictable dispersions and will not necessarily be indicative of an actual fiber cluster. Filtering based solely on points above the cutoff value is also susceptible to scanning window sensitivity.

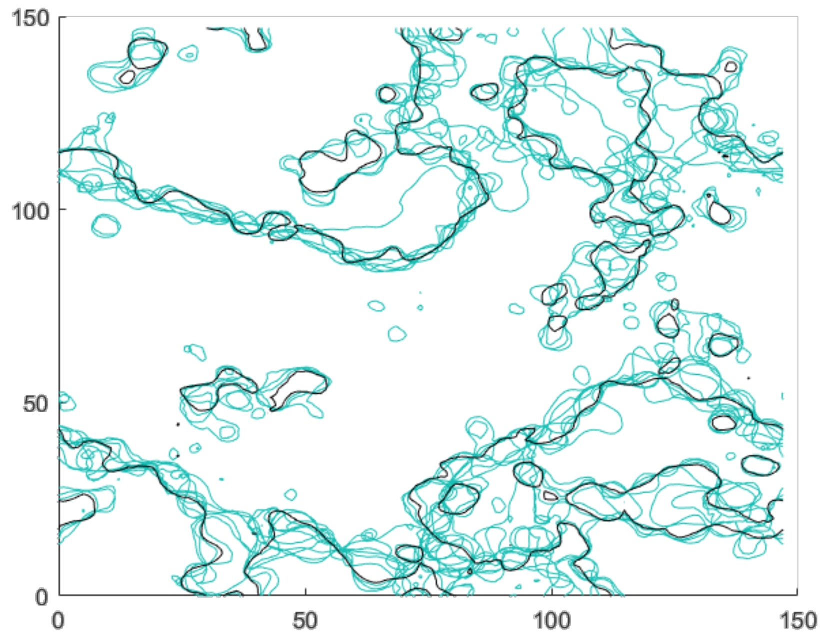

Figure 8.—Topology map of cluster boundary sensitivity to changing scanning window.

Figure 8 shows the boundary of clusters resulting from the cutoff plane intersecting with the volume fraction distribution (Figure 7). Each blue line represents a different scanning window radius ranging from ±2 µm from the scanning window size calculated using Equation (10). The black line represents the boundary from a window size that is determined from Equation (10). As seen from these boundaries, the cluster shape and size changes unpredictably, and inconsistently, at large deviations in scanning window size. Also, introduced with this variation is the formation of voids in the clusters at particular sizes. Lastly, it is difficult from this topology to determine a cluster shape and assign a specific geometry to calculate a cluster area. To overcome these problems, a filter is implemented which utilized triangulation and neighboring connections.

To filter the data for only significant contributing clusters, the RVE will first be discretized using Delaunay Triangulation which connects neighboring fibers to form a triangular grid. Triangulation is preformed to connected neighboring fiber centers, and based off previous thresholding, will dictate the initial cluster assignments. If a triangulation member has three vertices which all lie above the threshold, that triangle will be defined as “clustered”. This initial assignment will result in connected groupings of triangles which are all similarly assigned with some isolated and separated regions. The goal of filtering is to remove unconnected and isolated assignments while also filling in discontinuities in large connections while always ending up at a converged geometry. Filtering fibers in and out of the classification of being clustered is conducted by comparing not only the V_f of the current window but also the fiber volume fractions of the windows associated with adjacent fibers defined by the neighboring triangles.

1. Each triangle in Delaunay Triangulation will have three neighboring triangles. If the triangle being examined has less than two neighbors that are in a cluster, that triangle will be removed from the cluster.
2. If the triangle has two or more neighbors that is in a cluster, that triangle will remain part of the cluster, or will now be added to the cluster if not previously part of the cluster.

The filtering process operates under a loop where the triangulation is smoothed n times. The number of smoothing rounds is controlled by the user and will apply steps 1 and 2 of the procedure until triangles cannot be added nor subtracted. Figure 9 shows the result of an example microstructure in the final smoothing step where all possible triangles have either been filtered out or added. Triangles that have been filtered out are highlighted in green to denote that they are no longer part of the cluster, and only filled triangles (red) represent the final cluster shape and area.

Once the process has finished and all triangles have either been filtered out or added, there will be two final classifications. The first classification is the final cluster group which is composed of all the fiber coordinates which are part of the cluster and the triangulation area (red) that makes up the cluster area. The second classification is all area and points that have been either filtered out or were never classified as a cluster. These two classifications also make up the entire RVE area and will be used in further calculations.

As seen in Figure 9, not all points assigned clusters (red circles) or any filtered out triangles (green) are included in the final cluster shape. This filtering will only allow a cluster shape to be comprised of a minimum 4-5 triangles. It is theorized that disjointed parts extending from a cluster (green triangles) or relatively small clusters (red circles) removed from filtering will have negligible contribution not only to cluster statistics but also to the future RVE strength.

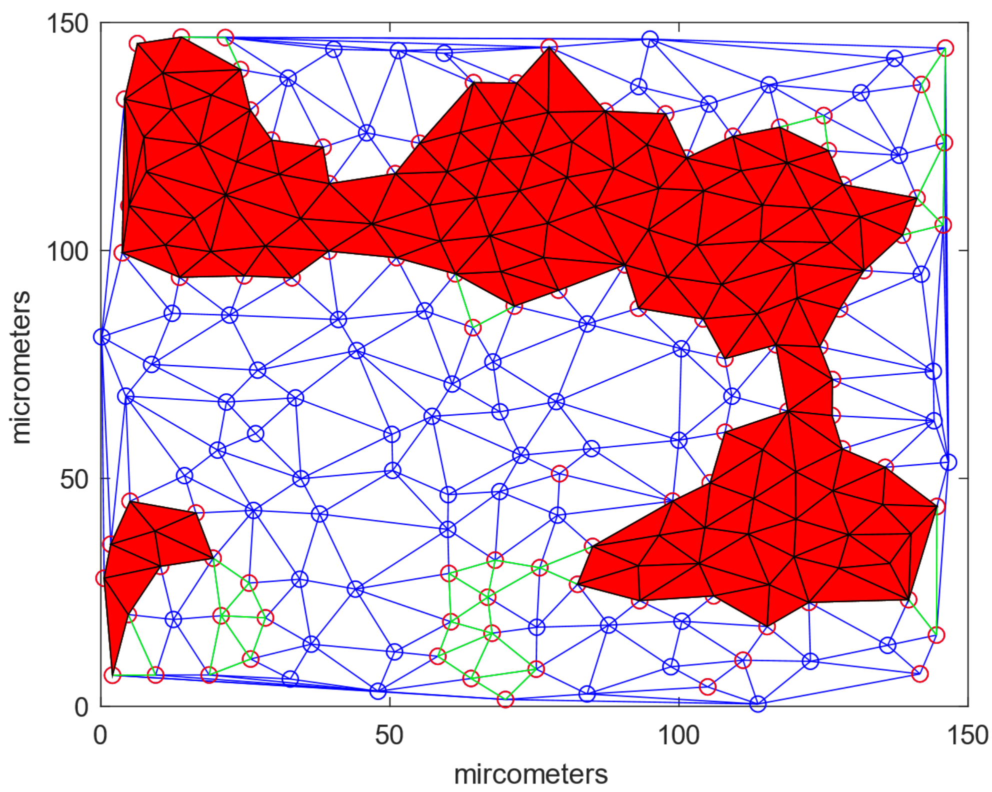

Figure 9.—Delaunay Triangulation of the whole RVE where red circles represent points above the cutoff value, blue circles represent points below the cutoff value, red triangles represent a cluster area, and green triangles represent cluster groups removed by filtering.

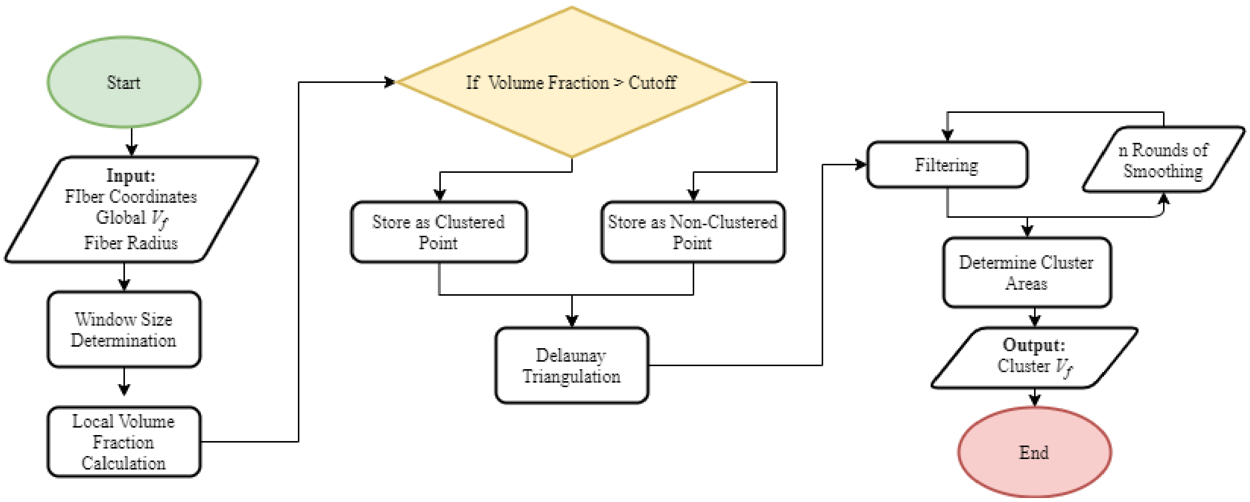

Figure 10.—Flowchart of final algorithm process.

2.3.2 Final Cluster Size and Application Process

The size of each cluster is taken by summing the area of clustered triangles. The size of each individual cluster is examined as well as the number of each cluster in the RVE. Summing all cluster areas and dividing by the total RVE area produces the cluster volume fraction for a sample shown in Equation (11).

$$V_{f_c} = \frac{\sum A_c^i}{A_{RVE}} \tag{11}$$

An algorithm with all presented processes and calculations is desired where a user can input specific parameters and output specific results.

Figure 10 depicts the final flowchart with all processes used in this algorithm. The process requires four inputs: fiber coordinates, global V_F, fiber radius, and rounds of smoothing. Descriptions of each process are calculated as described in previous sections. Calculation times can increase with the number of fibers in the RVE due to the proceeding area calculations and data storage during the Delaunay Triangulation filtering.

3.0 Results and Discussion

The purpose of this study is to create a method for efficient characterization of variability in fiber composite microstructures for classification of composite materials and virtual recreation of “as-manufactured” microstructures. In order to perform this analysis, DEM was used to generate RVEs with different levels of clustering. A parametric study was conducted on the contact damping in the DEM to evaluate its effect on clustering. The resulting samples were then analyzed by the scanning method described in the previous section. Finally, the novel scanning method introduced in this work, was used to characterize the clustering in a sample of composite material used in automotive applications.

3.1 Cluster Classification in Virtual RVEs

When generating microstructures using DEM, a concern is the possibility of overlapping fibers which are impossible in real samples. To ensure this does not occur, sufficient simulation time is allowed to dampen the kinetic energy, and all fibers approach a rest state.

The iterations of kinetic energy dispersion occur in equal increments of time. During relaxation, if a fiber moves out of the RVE it will be reflected to the opposite side. The final RVE shown in Figure 11 represents the final coordinates of fiber positions which will be used in the study.

It is desirable to identify the influence of the contact damping parameter in the DEM on the clustering in the RVE that is created. Therefore, real, as-manufactured microstructures, that have been characterized with respect to fiber aggregation, can be easily recreated virtually using DEM. Ten samples at a specified contact damping are generated, and the volume fraction of clusters in the RVE is calculated. Cluster volume fraction is calculated by the summation of the areas of all clustered triangles after filtering as defined by Equation (11). The global volume fraction of the samples is 40 percent and the scanning window size and cut off value are set accordingly, see Equation (10).

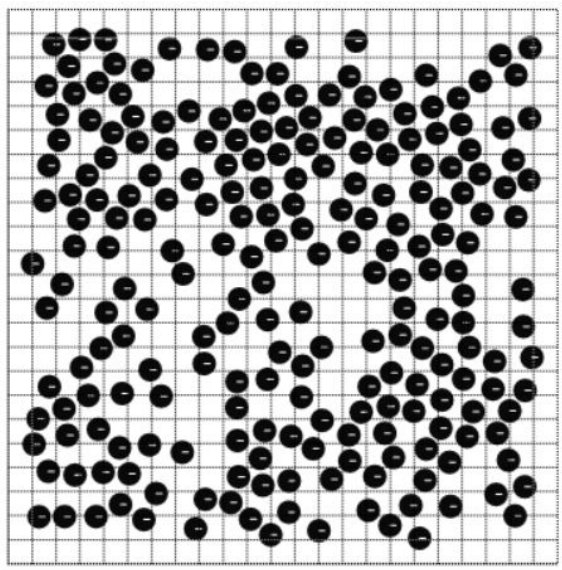

(a)

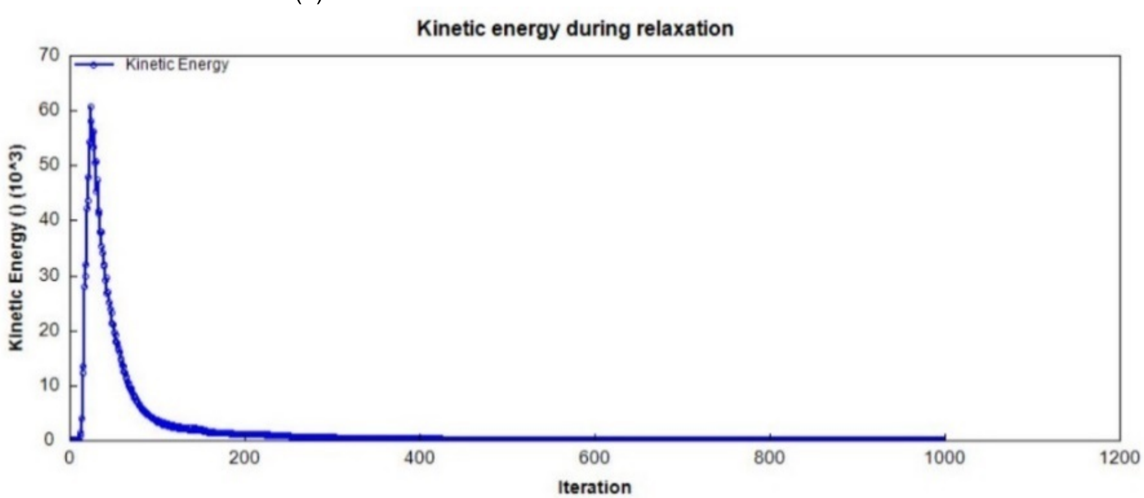

(b)

Figure 11.—Relaxation process for the (a) generated microstructure using (b) kinetic energy dispersion of the system as a function of fixed time iteration.

All simulations were performed on a standard laptop. To generate Figure 12, RVEs of 225 fibers were created and required an average total run time of 2.5 s per instance. For an increasing contact damping, the average cluster fraction increases to a maximum 42 percent and converges to slightly below 40 percent. The steepest increase in clustering is from a contact damping of 0.1 to 0.4, and the trend appears to be linear. Since convergence is occurring from 0.5, the maximum clustering from this parameter alone happens fairly fast. From Figure 12(a), there is more variation in lower contact damping such as 0.1.

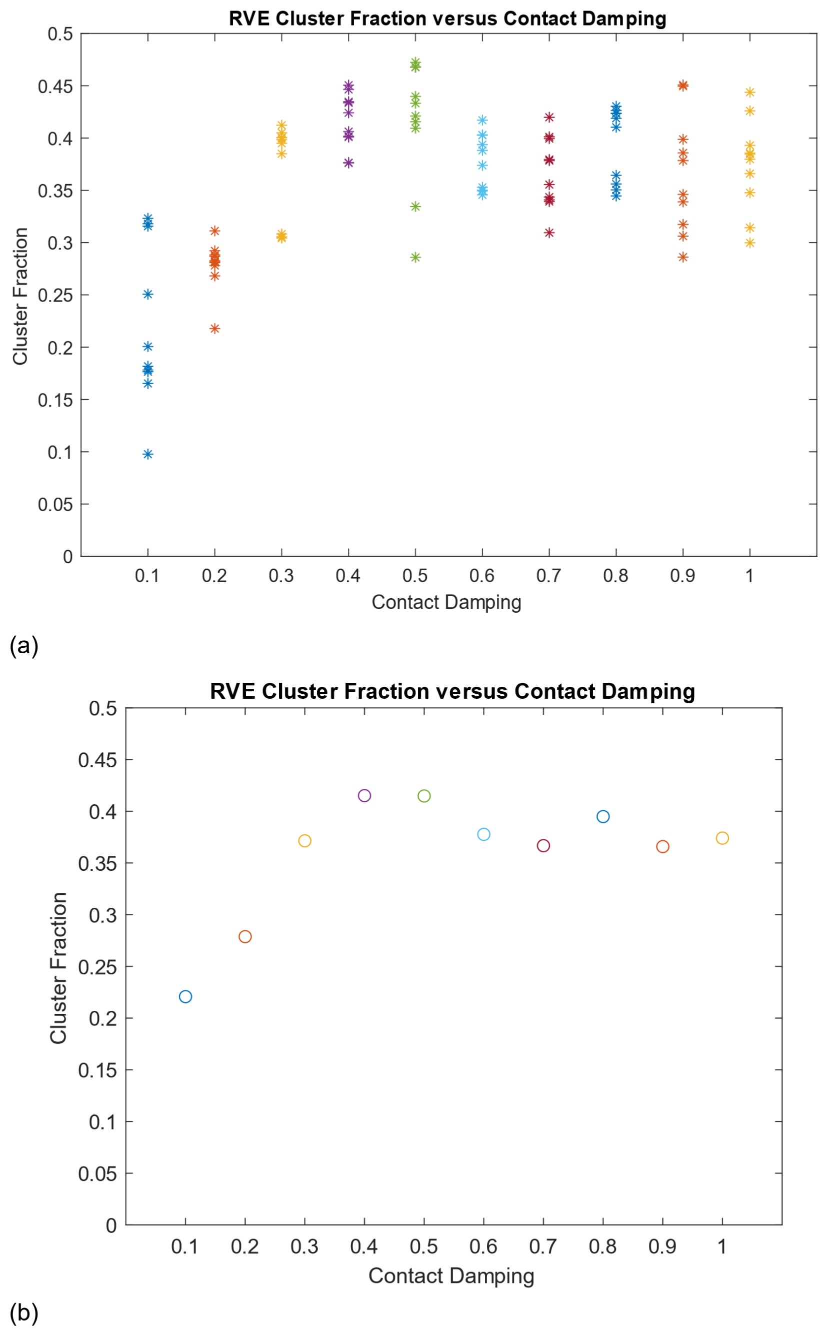

Figure 12.—(a) The individual results of ten samples generated for a specific contact damping. (b) The average cluster fraction of each contact damping group.

Figure 13 presented a SEM image of an automotive composite microstructure. Fiber coordinates were obtained through a greyscale analysis imported into the algorithm. The output of the clustering test is shown below in Figure 11. The known parameters of this composite sample are its volume fraction is approximately 40 percent, the total number of fibers is 3,429, and the fiber radius is 3.5 micrometers in average.

The resulting volume fraction of clusters within the sample is 41.11 percent with a total run time of 106.59 s. The only parameters adjusted for this experiment was to correspond the size of the scanning window to the global volume fraction and the fiber radius. The total processing time was ~90 s.

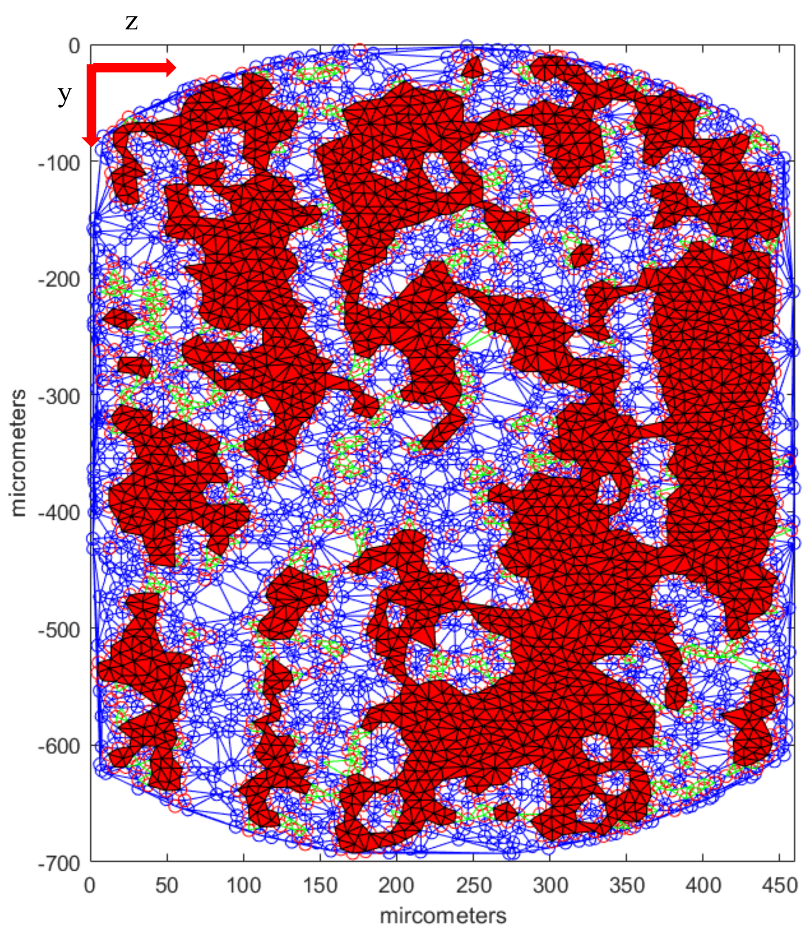

Figure 13.—Post process and clustering visualization of an actual composite microstructure. Every fiber coordinate is depicted as a point, blue points represent fibers not in a cluster and red points are fibers in a cluster. Red-filled triangles represent clustered points that make up a cluster. Blue and black lines represent the Delaunay Triangulation between coordinates. Green outlines triangles represent originally clustered triangles that were filtered out and are no longer part of a cluster.

4.0 Summary and Conclusions

The purpose of rapidly generating microstructures and evaluating the extent of fiber clustering is to ultimately enable a method for accurate generated models that are statistically equivalent to real, manufactured composites. Robust algorithms must be used in conjunction with fiber generation tools which can easily alter parameters to statistically correlate to microstructure scans. To characterize fiber dispersion and variability, the method of scanning for localized regions of high-volume fractions has been shown to be accurate and consistent. The algorithm evaluated in this work provides a meaningful step in rapid evaluation of composite microstructures. Currently, the algorithm is able to import fiber center locations, global volume fraction, and fiber radius and output the area of the clustering.

Future work will involve improving the algorithm to identify number of clusters, cluster shape, and cluster size. From these metrics, cluster centroids and densities can be determined, and the orientation of clusters be fitted. The overall goal of these modifications is to provide metrics by which clustering affects microstructure strength and how to capture local variability on a global scale.

There are multiple input parameters that control the DEM software, and each has a different influence on how the clusters are formed. Starting with one parameter, contact damping, where fibers lose kinetic energy through collisions it is seen for an RVE with a global volume fraction of 40 percent that contact damping has the greatest influence between settings of 0.1 and 0.5, after which the cluster fraction starts to saturate. The steep increase allows for minimal change in setting for a greater amount of clustering. To test new parameters, each will be tested individually as well as for their interaction. For instance, the corresponding influence that different types of damping may have on each other with respect to clustering can be studied. This algorithm proves to be a reliable and robust first step in characterizing localized regions of fiber distributions in composite microstructures.

References

1. Borkowski, Luke, Kuang C. Liu, and Aditi Chattopadhyay. "Micromechanics Model to Link Microstructural Variability to Fiber Reinforced Composite Behavior." In *55th AIAA/ASME/ASCE/AHS/ASC Structures, Structural Dynamics, and Materials Conference*. AIAA SciTech Forum. American Institute of Aeronautics and Astronautics, 2014. https://doi.org/10.2514/6.2014-0155.
2. González, E.V., P. Maimí, P.P. Camanho, C.S. Lopes, and N. Blanco. "Effects of Ply Clustering in Laminated Composite Plates under Low-Velocity Impact Loading." *Composites Science and Technology* 71, no. 6 (April 12, 2011): 805–17. https://doi.org/10.1016/j.compscitech.2010.12.018.
3. Mishnaevsky, Leon, and Gaoming Dai. "Hybrid Carbon/Glass Fiber Composites: Micromechanical Analysis of Structure–Damage Resistance Relationships." *Computational Materials Science* 81 (January 1, 2014): 630–40. https://doi.org/10.1016/j.commatsci.2013.08.024.
4. Li, Victor C., and Shuxin Wang. "Microstructure Variability and Macroscopic Composite Properties of High Performance Fiber Reinforced Cementitious Composites." *Probabilistic Engineering Mechanics*, Probability and Materials: from Nano- to Macro-Scale, 21, no. 3 (July 1, 2006): 201–6. https://doi.org/10.1016/j.probengmech.2005.10.008.
5. Bednarcyk, Brett A., Jacob Aboudi, and Steven M. Arnold. "Analysis of Fiber Clustering in Composite Materials Using High-Fidelity Multiscale Micromechanics." *International Journal of Solids and Structures* 69–70 (September 1, 2015): 311–27. https://doi.org/10.1016/j.ijsolstr.2015.05.019.

6. Pathan, M.V., V.L. Tagarielli, S. Patsias, and P.M. Baiz-Villafranca. "A New Algorithm to Generate Representative Volume Elements of Composites with Cylindrical or Spherical Fillers." *Composites Part B: Engineering* 110 (February 1, 2017): 267–78. https://doi.org/10.1016/j.compositesb.2016.10.078.
7. Mishra, B.K., and Raj K. Rajamani. "The Discrete Element Method for the Simulation of Ball Mills." *Applied Mathematical Modelling* 16, no. 11 (November 1, 1992): 598–604. https://doi.org/10.1016/0307-904X(92)90035-2.
8. Baddeley, Adrian. "Spatial Point Processes and Their Applications," n.d., 75.
9. El-Shaarawi, A.H., and Walter W. Piegorsch, eds. *Encyclopedia of Environmetrics*. Chichester ; New York: Wiley, 2002.
10. "Modelling Spatial Patterns Author(s): B.D. Ripley Source: Journal of the Royal Statistical Society. Series B (Methodological), Vol. 39 - Google Search." Accessed January 5, 2020. https://www.google.com/search?q=Modelling+Spatial+Patterns+Author(s)%3A+B.+D.+Ripley+Source%3A+Journal+of+the+Royal+Statistical+Society.+Series+B+(Methodological)%2C+Vol.+39&oq=Modelling+Spatial+Patterns+Author(s)%3A+B.+D.+Ripley+Source%3A++Journal+of+the+Royal+Statistical+Society.+Series+B+(Methodological)%2C+Vol.+39&aqs=chrome..69i57.1086j0j7&sourceid=chrome&ie=UTF-8.
11. Ripley, B.D. "Modelling Spatial Patterns." *Journal of the Royal Statistical Society: Series B (Methodological)* 39, no. 2 (1977): 172–92. https://doi.org/10.1111/j.2517-6161.1977.tb01615.x.
12. Teichmann, Jakob, Felix Ballani, and Karl Gerald van den Boogaart. "Generalizations of Mat\'ern's Hard-Core Point Processes." *ArXiv:1209.2566 [Math, Stat]*, September 12, 2012. http://arxiv.org/abs/1209.2566.
13. Kwon, Young, David H. Allen, and Ramesh R. Talreja. *Multiscale Modeling and Simulation of Composite Materials and Structures*. Springer Science & Business Media, 2007.
14. Liu, Kuang C., and Anindya Ghoshal. "Validity of Random Microstructures Simulation in Fiber-Reinforced Composite Materials." *Composites Part B: Engineering* 57 (February 1, 2014): 56–70. https://doi.org/10.1016/j.compositesb.2013.08.006.
15. Romanov, Valentin, Stepan V. Lomov, Yentl Swolfs, Svetlana Orlova, Larissa Gorbatikh, and Ignaas Verpoest. "Statistical Analysis of Real and Simulated Fibre Arrangements in Unidirectional Composites." *Composites Science and Technology* 87 (October 18, 2013): 126–34. https://doi.org/10.1016/j.compscitech.2013.07.030.
16. Elnekhaily, S.A., and Talreja, R., "Damage initiation in unidirectional fiber composites with different degrees of nonuniform fiber distribution," *Composites Science and Technology*, vol. 155, 2018, pp. 22–32.
17. Stapleton, Appel, Simon, and Reese S. "Representative Volume Element for Parallel Fiber Bundles: Model and Size Convergence." *Composites: Part A* (April 16, 2016)[17] Pschel T, Schwager T. Computational Granular Dynamics. Springer, 2005.
18. Radjai F., Dubois F., Discrete-element modeling of granular materials. Wiley-Blackwell; 2011.
19. Luding S. Introduction to discrete element methods: basic of contact force models and how to perform the micro-macro transition to continuum theory. Eur J Environ Civ Eng 2008; 12(7): 785–826.